

Anticorrosive Performance of Commercial Nanoceramic Coatings on AISI 1010 Steel

Estela Knopp Kerstner^a, Sandra Raquel Kuns^a, Lilian Vanessa Rossa Beltrami^a,

Maria Rita Ortega Vega^a, Lisete Cirstina Scienza^b, Célia de Fraga Malfatti^{a}*

^a*Laboratório de Pesquisa em Corrosão – LAPEC, Programa de Pós-Graduação em Engenharia de Minas, Metalúrgica e de Materiais – PPGEM, Universidade Federal do Rio Grande do Sul – UFRGS, Porto Alegre, RS, Brazil*

^b*Laboratório de Corrosão - Pesquisa – LACORP, Programa de Pós-Graduação em Engenharia de Processos e Tecnologias – PGEPROTEC, Universidade de Caxias do Sul – UCS, Caxias do Sul, RS, Brazil*

Received: January 15, 2014; Revised: September 11, 2014

The aim of this work was to study the corrosion behavior of three commercial nanoceramic coatings in comparison to zinc phosphate coatings applied on mild steel (SAE 1010). The coatings were evaluated by scanning electron microscopy (SEM), profilometry and hydrophobicity. The electrochemical behavior was evaluated by dynamic polarization. The results showed that the samples coated with nanoceramics presented contact angles greater than 100°, achieving hydrophobic behavior. Evaluating the electrochemical behavior under dynamic polarization revealed that the nanoceramic coating containing chromium (CHT) exhibited a higher corrosion potential and lower current than the other nanoceramic coatings tested, although its performance in a dilute sodium chloride solution was below that of the zinc phosphate-based coating. Although the nanoceramic coatings exhibited poor electrochemical behavior compared to the zinc-based coatings, they had a higher corrosion resistance when associated with an organic coating.

Keywords: *corrosion, steel, nanoceramic coatings, zinc phosphate*

1. Introduction

The corrosion of metallic materials causes many industrial problems, decreasing equipment life spans and leading to their maintenance or even replacement and, costing time and money¹.

Protective coatings are used on metal materials to inhibit corrosion and to preserve the materials. The coating materials can be metals, ceramics, polymers, or combinations thereof, and their selection depends on the design requirements and the coating application².

The phosphating process is the most widely used metal pretreatment process for ferrous substrates³, and has been used for various applications in many industrial fields⁴. The most important application of the phosphating process is as a pretreatment for finishing paint, where it increases the film adhesion to the substrate, improving the paint barrier effect, thus avoiding the subcutaneous corrosion progress. Studies show that the resistance corrosion performance of painted metals is approximately 700 times greater when the metal is phosphatized prior to painting⁵.

Little research has been conducted to find alternative processes to phosphate coatings. The study by Li et al.⁶ presented an alternative method to phosphate pretreatment based on Mn-Zn, which is free of hazardous compounds such as nitrides, chromium and nickel. According to the authors, this pretreatment resulted in a high level of adhesion

to the substrate, good uniformity, and effective protection against corrosion.

Nanoceramic coatings are promising alternatives to phosphate coatings⁷⁻⁹, with numerous industrial applications, mainly due to their high resistance to wear and erosion, protection against corrosion, and thermal insulation³. This new process allows for the production of nanometer scale coatings of metal substrates (iron, steel, zinc, and aluminum) based on a combination of a nano-structured metal oxide type ceramic with metals such as titanium and/or zirconium^{10,11}. Nanoceramics are thin, uniform layers with special properties that enable the coatings to be painted such as adhesion, flexibility and increased corrosion resistance compared to iron phosphate and zinc¹².

This work aims to investigate commercial nanoceramic coatings and to compare their properties with the conventional zinc phosphating process using 1010 steel as the substrate.

2. Experimental

This work used AISI 1010 steel panels as the substrate (dimensions of 50 × 177 × 0.45 mm thick), with the following chemical composition: 0.1014 C, 0.01 Si, 0.42 Mn, 0.01 P, 0.007 S, 0.033 Al and 0.011 Cr (in wt%). Three commercial nanoceramics formulations (without phosphates) were used, and a commercial phosphatizing solution based on zinc phosphate was used for surface

*e-mail: celia.malfatti@ufrgs.br

pretreatment (Table 1). The operating parameters followed the manufacturer's recommendations.

The samples were characterized by scanning electron microscopy (SEM) using a JEOL 6060 microscope. The surface wettability was determined by contact angle measurements, using the sessile drop method.

The electrochemical polarization test was carried out with a potentiostat/galvanostat Autolab and a conventional three-electrode cell: the sample was set as a working electrode, a platinum electrode acting as an auxiliary electrode and the reference electrode a saturated calomel electrode (SCE). A 0.01 M NaCl solution (pH~6) was used as the electrolyte (STP Conditions). A 0.626 cm² area was analyzed.

It is applied a black powder polyester paint on the pretreated samples to evaluate the effect the combination of the pretreatment with organic coating. The paint application was made in the cabin containing an electrostatic system (brand Erzinger) using a flow rate of 1.5 m³.h⁻¹ and 80 kV voltage, after the samples were cured in an oven for 20

minutes at 200 °C. The layer thickness paint was measured at three different points and was calculated averaged.

The adhesion, impact and flexibility tests the samples pretreated and painted was performed in accordance to ASTM D3359-09¹³, ASTM D 2794-99¹⁴ and ABNT NBR 10545-88¹⁵, respectively.

The test evaluation of corrosion was based on ASTM B 117-07¹⁶, performed in a salt spray chamber (YU Heng Instrument Co. LTD, model HY-952b Salt Spray Tester), where the painted panels were placed 15° from the vertical position, with total time of 1272 hours of exposure, with evaluation performed every 24 hour cycle. The painted samples were characterized by corrosion behavior according to ASTM D 714-02¹⁷ and ASTM D 610-08¹⁸ standards that evaluate the evolution of the degree of rusting and blistering of painted surfaces respectively.

Figure 1 shows the sequence of steps taken the development of this study and the characterization tests performed on the samples.

Table 1. Description of the samples.

| Sample | Description | Operational parameters | | |
|--------|--|---|------------------|----------|
| | | Concentration (%v/v) | Temperature (°C) | Time (s) |
| BR | Blank reference | --- | --- | --- |
| CHT | Nanoceramic trivalent chromium based | 3 | 23-25 | 60 |
| AFZ | Nanoceramic fluorzirconium acid based | 3 | 23-25 | 60 |
| AHFZ | Nanoceramic hexafluorizirconium acid based | 6 | 23-25 | 60 |
| ZPH | Coating zinc phosphate based | A = 70 (g.L ⁻¹) B = 1.6 (g.L ⁻¹) | 27 | 300 |

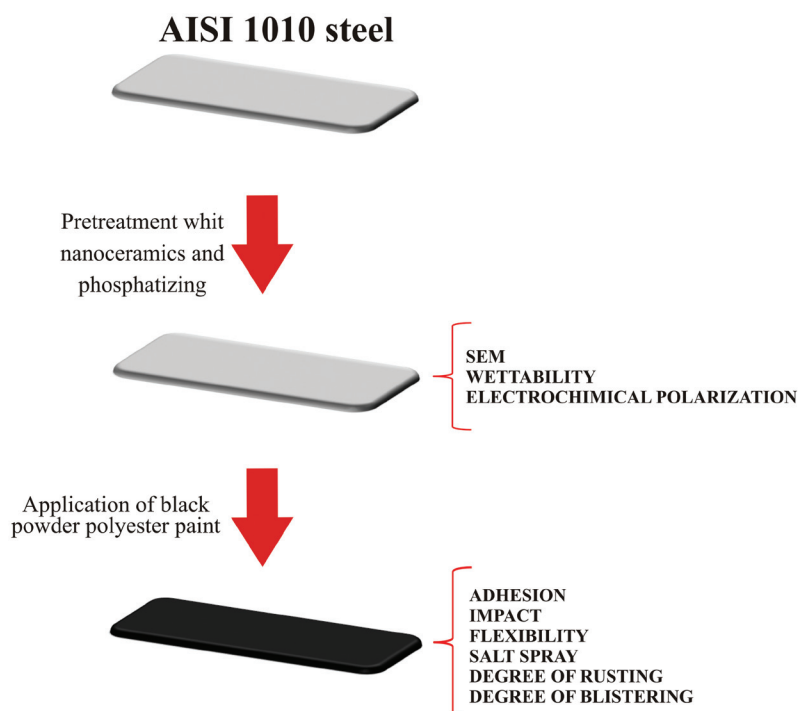


Figure 1. Schematic illustration of steps and tests.

3. Results and Discussion

The SEM micrographs (Figure 2) demonstrated that the CHT sample (Figure 2b) exhibited a uniform layer covering the surface, with protuberances observed on the surface.

The AHFZ and AFZ samples (Figure 2c-d) also present a uniform layer covering their surfaces, with small granular deposits distributed throughout the surface. The ZPH sample (Figure 2e) presents a uniform phosphated coating formed by irregular lamellar crystals. According to Banczek et al. and Moore et al.¹⁹⁻²⁰, the morphology observed in the phosphate sample is common due to the formation of hopeite, which consists of hydrated zinc phosphate ($Zn_3(PO_4)_2 \cdot 2H_2O$)¹⁹⁻²⁰.

Figure 3 shows the images obtained for the contact angle measurements by the sessile drop method. The nanoceramic coating samples (Figure 3b-d) exhibited contact angles over 100° , indicating hydrophobic surface behavior. Hydrophobic surfaces are considered anti-corrosives because they repel water, minimizing the corrosion electrochemical reaction²¹. Among the coatings tested here, the AFZ sample (Figure 3c) showed the highest contact angle, indicating the lowest wettability.

Studies show that wettability can be directly influenced by the surface roughness, with an inversely proportional ratio between them²²⁻²⁴. However, it is important to consider that in addition to morphology, surface composition also influences the wettability of the substrate²⁵⁻²⁶. Thus, whereas the roughness observed for systems pre-treatments studied was very similar, and that the chemical composition of these is distinct, can assume that the difference in wettability is

influenced by the chemical composition of the film formed. The ZPH sample (Figure 3d) showed a lower contact angle (lower than 90°), indicating a higher wettability (hydrophilic behavior), while all the nanoceramic coatings presented contact angles of approximately 100° (hydrophobic behavior). This result indicates that the nanoceramic coating contributes to increasing the surface hydrophobicity.

Figure 4 is present the open circuit potential (OCP) monitored for one hour. The CHT pretreated material exhibited an initial decrease in potential, possibly due to the presence of defects in the coating, followed by a small stable potential range, indicating that corrosion products block further corrosive action. After the corrosion products are dissolved in solution, a new and permanent corrosive attack occurs. For the AFZ and AHFZ coatings, the corrosive attack occurs swiftly and intensely, as indicated by the active potentials observed for these systems during OCP monitoring. ZPH pretreatment at less active potential compared to the nanoceramic coating, exhibiting the best electrochemical behavior in terms of open circuit potential.

Figure 5 shows the polarization curves and Table 2 presents the corrosion density current values (i_{corr}), corrosion potential values (E_{corr}) and polarization resistance values (R_p), obtained by a Tafel simulation from the polarization curves.

The ZPH coating followed by the nanoceramic CHT coating exhibition lower i_{corr} values and higher E_{corr} and R_p values compared to the two other nanoceramic coatings AFZ (fluor-zirconium acid based nanoceramic) and AHFZ (hexafluor-zirconium acid based nanoceramic), which exhibit similar behavior. This result demonstrates the effect of

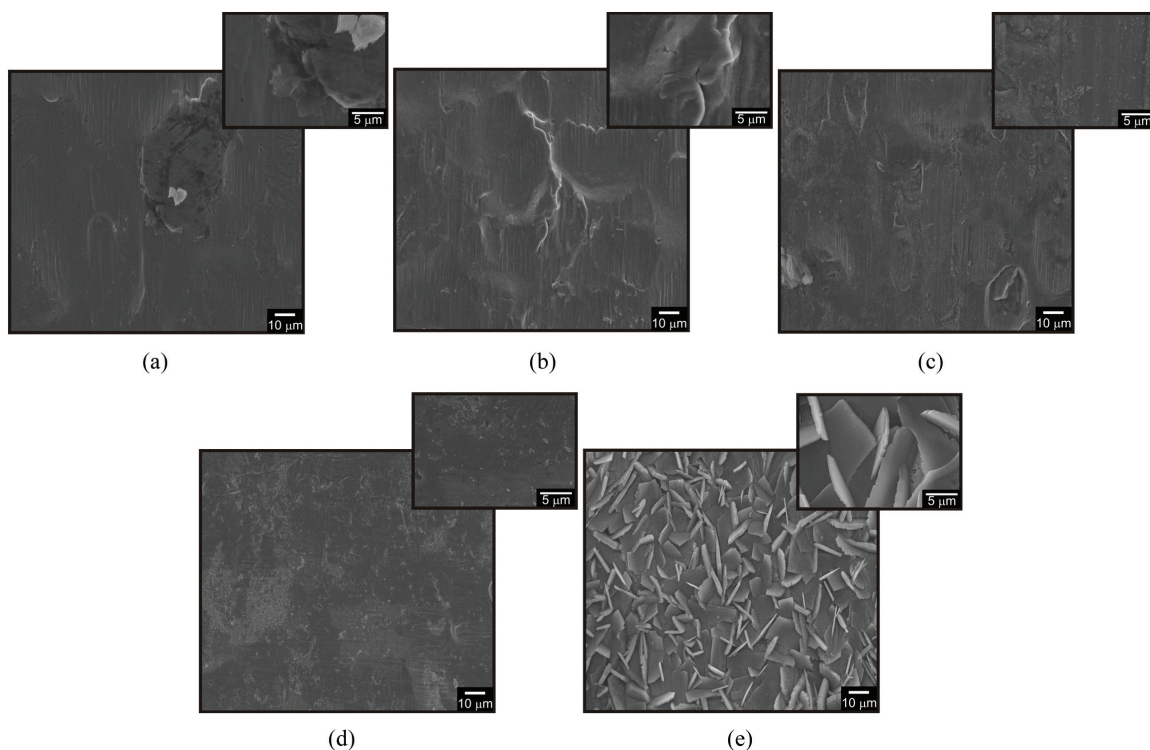


Figure 2. SEM samples with different pretreatments: (a) BR, (b) CHT, (c) AFZ, (d) AHFZ and (e) ZPH, with magnitude of 1,000x and 5,000x.

the coating composition on the corrosion performance of pretreatment coatings and shows that the best protective behavior is conferred to the substrate pretreated with zinc phosphate and trivalent chromium based nanoceramic.

Figure 6 shows the SEM images of the samples after the electrochemical potentiodynamic polarization test. The CHT sample (Figure 6b) presented is attacked uniformly due to the presence of cracks in the coating. Cracks were observed

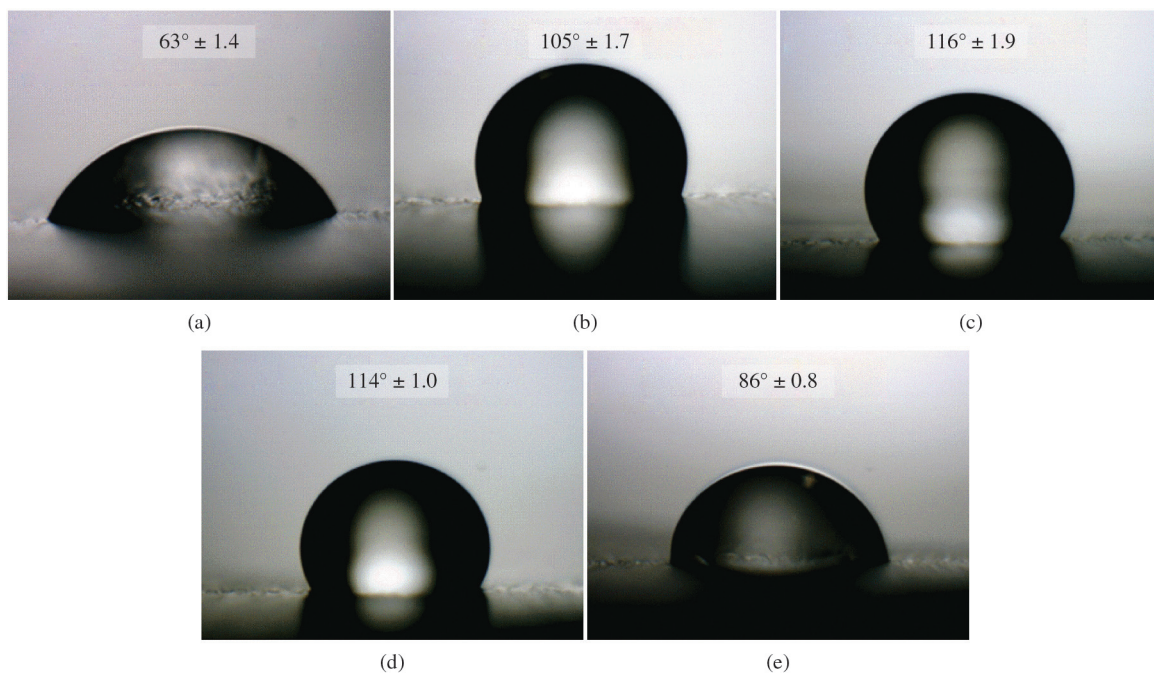


Figure 3. Contact angle measurements by the sessile drop method for the different pre-treatments: (a) BR, (b) CHT, (c) AFZ, (d) AHFZ and (e) ZPH.

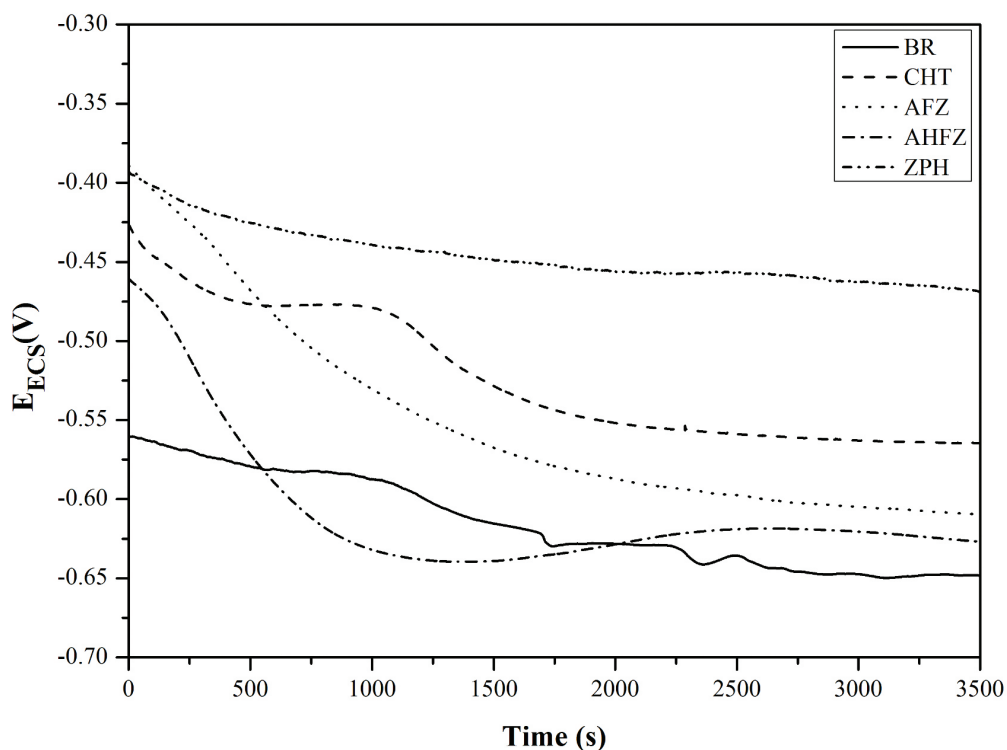


Figure 4. OCP diagram (in a 0.01 M NaCl solution) for pretreated samples.

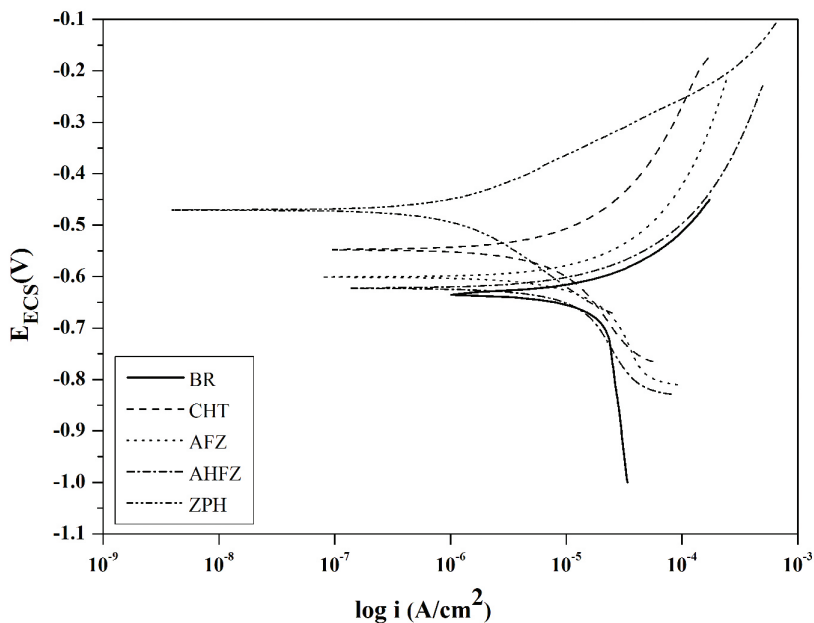


Figure 5. Anodic and cathodic polarization curves (in a 0.01 M NaCl solution) for pretreated samples.

Table 2. Values of parameters obtained from the simulation of the Tafel slopes.

| Sample | i_{corr} (A.cm ⁻²) | E_{corr} (V) | R_p (Ω.cm ²) |
|--------|----------------------------------|----------------|----------------------------|
| BR | 1.01E-6 | - 0.637 | 1,25E+4 |
| CHT | 9.70E-5 | - 0.549 | 4.57E+3 |
| AFZ | 1.96E-4 | - 0.602 | 2.41E+3 |
| AHFZ | 1.01E-4 | - 0.623 | 2.21E+3 |
| ZPH | 1.89E-6 | - 0.470 | 2.29E+4 |

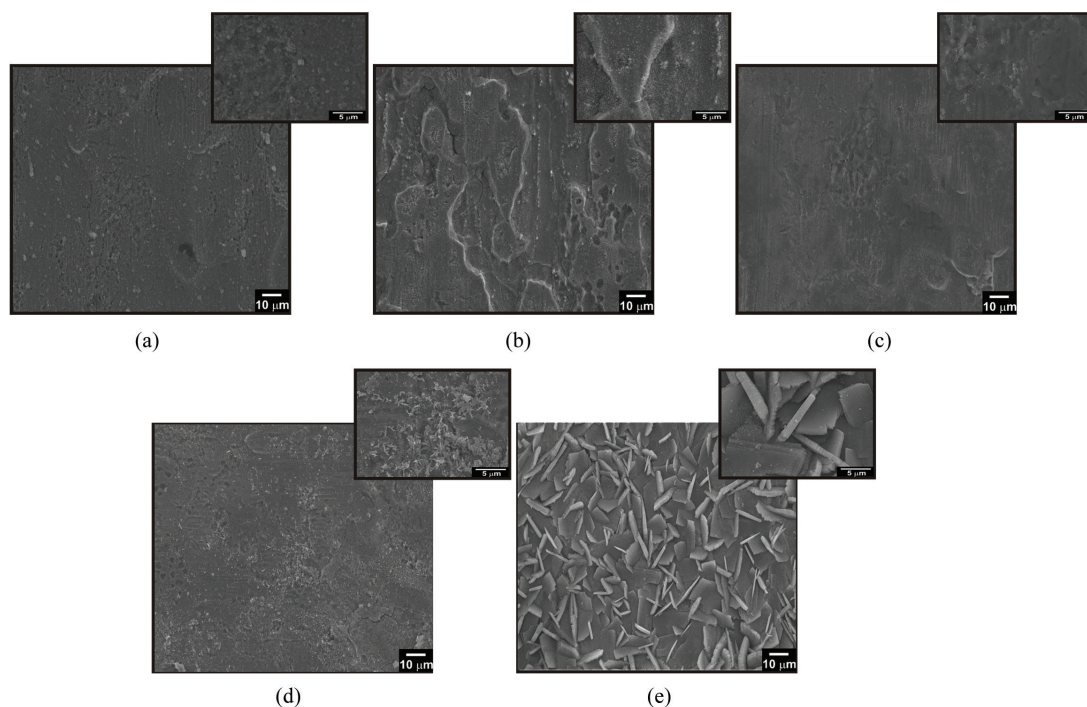


Figure 6. SEM samples with different pretreatments after electrochemical tests: (a) BR, (b) CHT, (c) AFZ, (d) AHFZ and (e) ZPH, with magnitude of 1,000x and 5,000x.

on the surface of the AFZ sample (Figure 6c), as well as the presence of clusters of corrosion products. The AHFZ sample (Figure 6d) exhibits surface porosity, the presence of cracks, and the formation of a large amount of corrosion products. For the ZPH sample (Figure 6e), the integrity of the pretreated coating was not affected in this experiment, with the film remaining even and without imperfections.

Table 3 shows the average thickness of the paint layer applied to the pretreated samples.

The adhesion test is intended to determine the adhesion between the paint and the metal substrate with different pretreatments. According to the classification the ASTM D3359-09¹³, the adhesion observed refers to the 6B scale, where the edges of the cuts are completely smooth and none of the squares of the lattice is detached (Figure 7), featuring a perfect adherence.

Table 3. Average thickness of the paint layer applied to the pretreated samples

| Sample | Thickness (μm) |
|--------|-----------------------------|
| BR | 69 ± 3 |
| CHT | 68 ± 8 |
| AFZ | 72 ± 1 |
| AHFZ | 81 ± 3 |
| ZPH | 74 ± 7 |

The impact (Figure 8) and flexibility tests (Figure 9) showed similar performance between the pre-treatments, for all samples kept paint adhesion, with no cracks and less points detachment.

After exposure of 1272 hours salt spray, there is a significant difference in corrosion performance for samples painted for different employees pretreatments when evaluated according to the degree of blistering and rusting (Figure 10). The Table 4 shows the results the formation of the blistering throughout the period of exposure to salt spray.

It was found that the blistering degree was more intense in the ZPH sample, since the first 168 hours observed the appearance of blistering and during the test were intensifying reaching the classification D-2 (size 2 and dense distribution).

In their study Bajat et al.²⁷ highlighted the importance of the roughness and the fostering phosphate based pretreatment on the formation of stronger bonds with polyester based coating. However the results of their study showed that the sample with phosphate coating painted with polyester resin showed no stability when exposed to a corrosive environment, showing similar behavior to the results obtained in this work.

Adhikari et al.²⁸ studied adhesion and corrosion the aluminum substrates with pretreatments the zirconia based and the phosphate based in epoxy paint. The results show that when aluminum-coated surface is exposed to an aqueous environment the water molecules penetrate through the

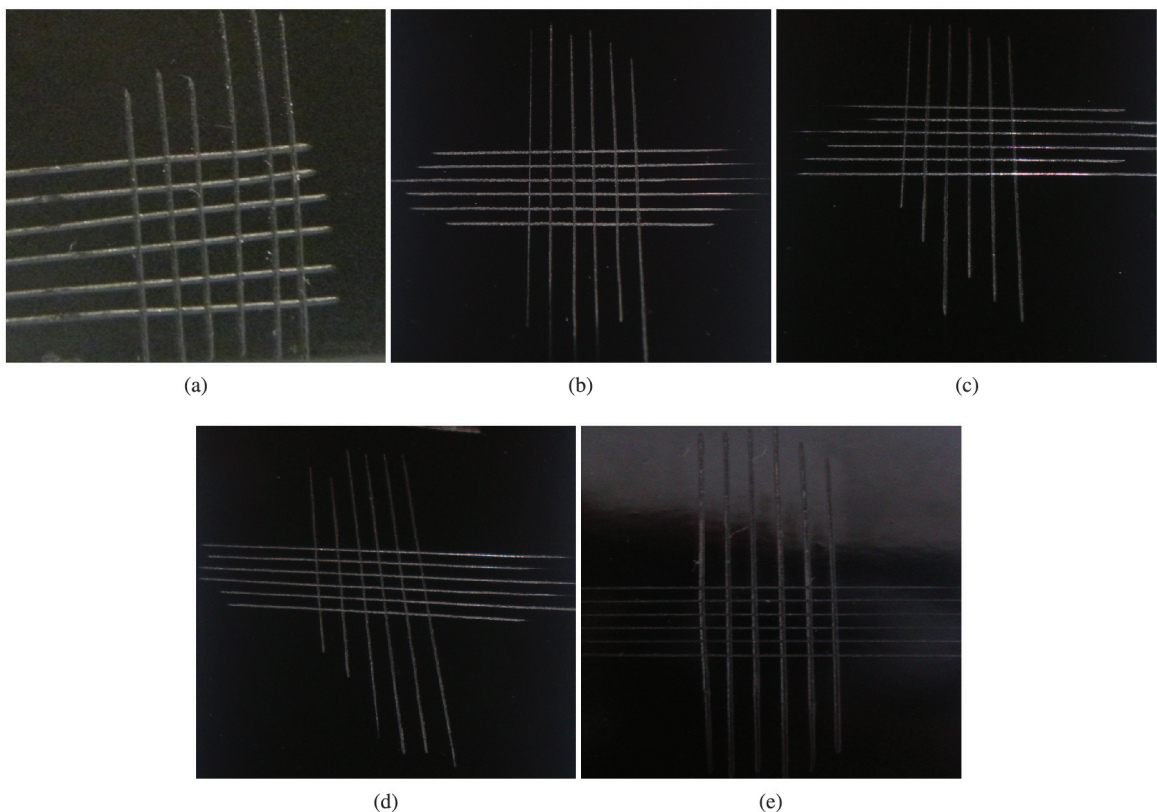


Figure 7. Pictures the samples subjected to adhesion test (a) BR, (b) CHT, (c) AFZ, (d) AHFZ and (e) ZPH.

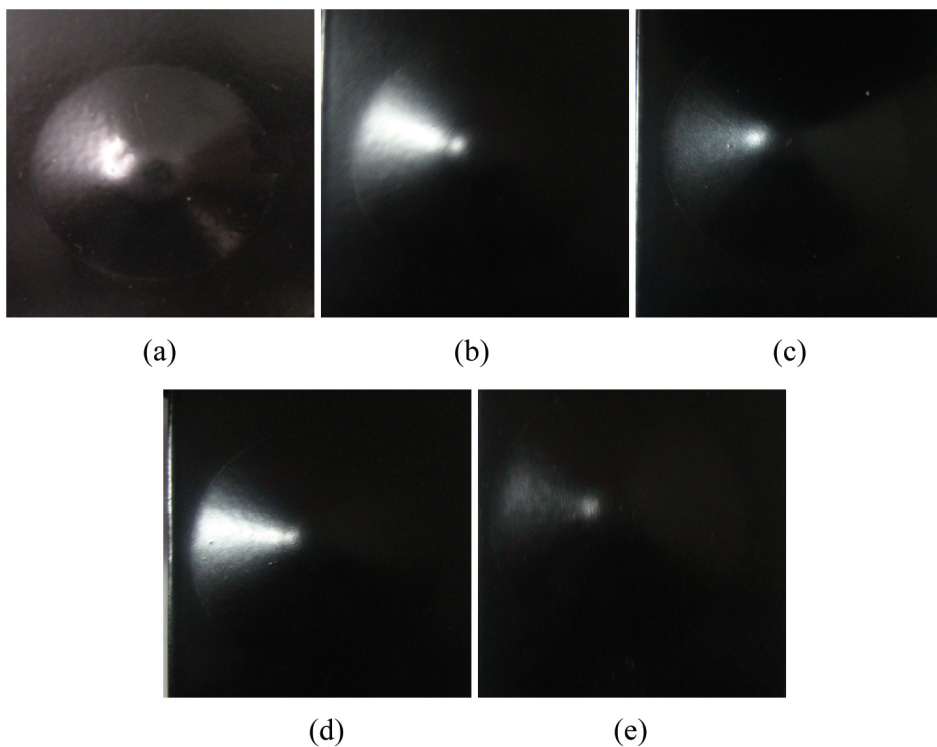


Figure 8. Impact test for the samples: (a) BR, (b) CHT, (c) AFZ, (d) AHFZ and (e) ZPH.

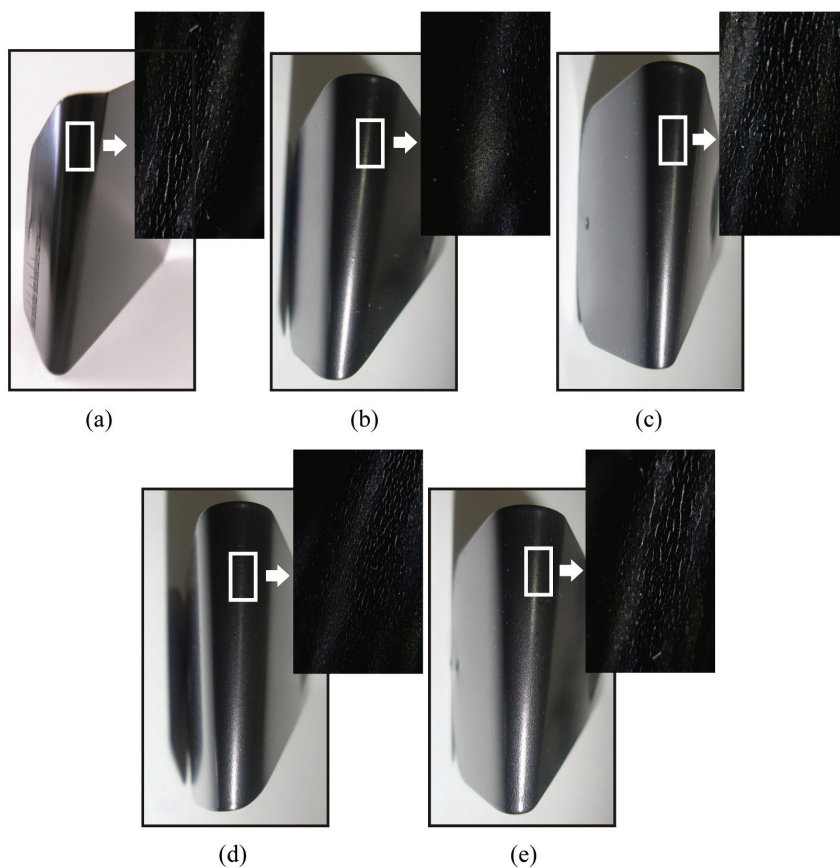


Figure 9. Flexibility test for the samples: (a) BR, (b) CHT, (c) AFZ, (d) AHFZ and (e) ZPH.

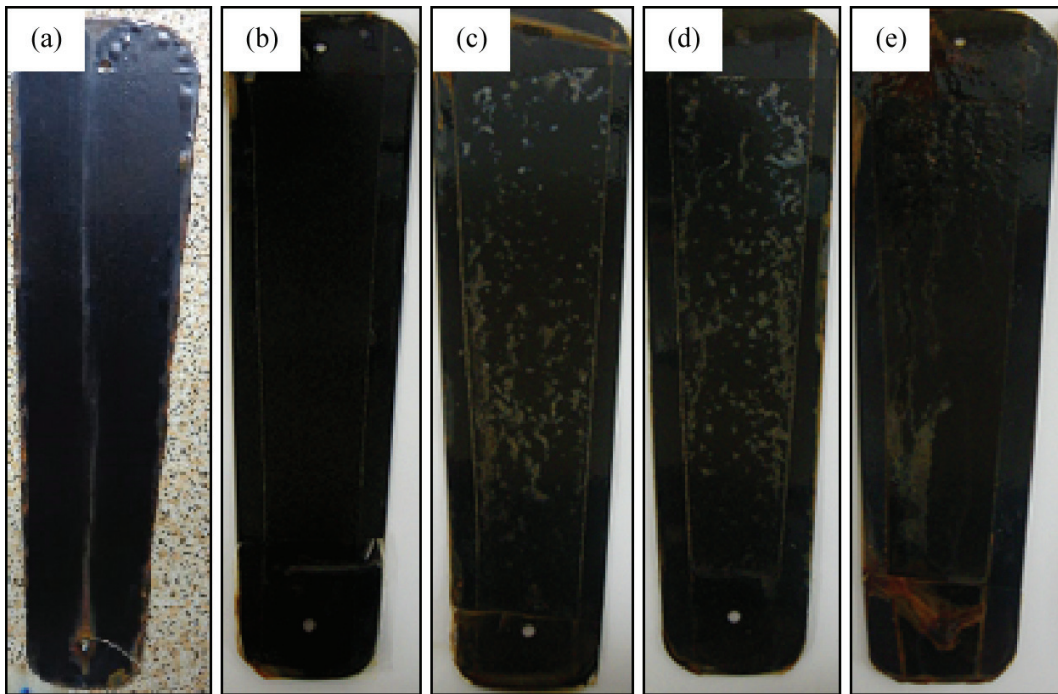


Figure 10. Blistering and rusting for the samples: (a) BR, (b) CHT, (c) AFZ, (d) AHFZ and (e) ZPH, after 1272 of exposure to salt spray.

Table 4. Blistering of the samples after salt spray.

| Time (h) | BR | CHT | AFZ | AHFZ | ZPH |
|----------|------|------|------|------|----------|
| 24 | F-10 | F-10 | F-10 | F-10 | F-10 |
| 168 | F-10 | F-10 | F-10 | F-10 | F-4 |
| 360 | F-10 | F-10 | F-10 | F-10 | M-2 |
| 504 | F-10 | F-10 | F-10 | F-10 | F-6 M-2 |
| 696 | F-10 | F-10 | F-4 | F-10 | F-6 MD-2 |
| 840 | F-10 | F-10 | M-4 | F-4 | F-6 MD-2 |
| 1032 | F-10 | F-10 | M-4 | F-4 | D-2 |
| 1176 | F-10 | F-10 | M-4 | F-4 | D-2 |
| 1272 | MD-2 | F-10 | M-4 | M-4 | D-2 |

Legend: Frequency of blistering: D - Dense; MD - Medium dense; M - Medium and F - Few. Size blisters: n° 10 represent no blistering; n° 8 represent smallest size blister easily seen by the unaided eye and blistering standards n° 6, 4, and 2 represent progressively larger sizes.

coating and accumulate in the coating/substrate interface, resulting in decreased adhesion strength and subsequent delamination of the paint layer.

Coatings nanoceramics showed lower degree blistering, and the CHT sample showed the best performance, with zero degree blistering. It was observed in the AFZ and AHFZ samples the formation of some medium blisters distributed over the whole surface.

Table 5 shows the results of the evaluation of rusting during the period of exposure to salt spray.

Observed appearance of corrosion points occurred in the AFZ and AHFZ samples after 504 hours and in the CHT sample in 1032 hours. It was observed in some samples the stabilization of these points of corrosion, but in others these have spread throughout the surface analysis. In the ending test the AFZ and AHFZ samples presenting the highest degree of rust, indicating greater severity of the corrosion.

It was observed the appearance the corrosion points in the ZPH sample after 72 hours; however along the exposure to salt spray, the rust was less intense than in nanoceramics samples.

Organic coatings provide corrosion protection acting as a barrier between the substrate and the environment. However, depending on coating thickness, substrate type, treatment applied to the surface and of the exposure time and the composition of the medium, these coatings present levels of permeability to water and oxygen²⁹, which promotes corrosion the metal substrate.

All samples showed formation of corrosion but not observed a relation between the thicknesses of the paint layer with corrosion resistance, since the sample CHT showed better corrosion protective performance even with less thickness paint.

Table 5. Rusting of the samples after salt spray.

| Time (h) | BR | CHT | AFZ | AHFZ | ZPH |
|----------|-----|-------|-----|-------|-----|
| 24 | 10 | 10 | 10 | 10 | 10 |
| 72 | 10 | 10 | 10 | 10 | 9S |
| 168 | 10 | 10 | 10 | 10 | 9S |
| 360 | 10 | 10 | 10 | 10 | 9S |
| 504 | 10 | 10 | 9S | 8S | 7S |
| 696 | 10 | 10 | 8S | 7G 9S | 7S |
| 840 | 10 | 10 | 6G | 7G 4S | 5S |
| 1032 | 10 | 8S | 6G | 7G 4S | 5S |
| 1176 | 10 | 4S 6G | 4G | 4G 4S | 5S |
| 1272 | 10P | 6S 6G | 3G | 4G 4S | 4S |

Legend: Rust grade of surface: Spot (S), General (G) and Pinpoint (P). Percent of surface rusted: 10 (<0.01%), 9 (0.01 – 0.03%), 8 (0.03 – 0.1%), 7 (0.1 – 0.3%), 6 (0.3 – 1.0%), 5 (1.0 – 3.0%), 4 (3.0 – 10.0%), 3 (10.0 – 16.0%), 2 (16.0 – 33.0%), 1 (33.0 – 50.0%) and 0 (> 50.0%).

4. Conclusions

The results obtained in this work showed that nanoceramic coatings exhibited contact angles greater than 90°, indicating hydrophobic behavior. The zinc phosphate sample presented a higher open circuit potential, with lower current density values and higher corrosion potential values, presenting the best electrochemical behavior.

The CHT sample exhibits the best performance among the coatings tested here. This result confirms, that the

chemical composition of the coating is extremely important, as chromium compounds are corrosion inhibitors and act by blocking the corrosive action at the metal/coating interface.

Acknowledgements

The present work was carried out with support of CAPES and CNPQ, Brazilian Government entity focused in human resources formation.

References

- El-Amoush AS, Abu-Rob A, Edwan H, Atrash K and Igab M. Tribological properties of hard chromium coated 1010 mild steel under different sliding distances. *Solid State Sciences*. 2011; 13(3):529-533. <http://dx.doi.org/10.1016/j.solidstatesciences.2010.12.020>.
- Sá Brito VRS, Bastos IN and Costa HRM. Corrosion resistance and characterization of metallic coatings deposited by thermal spray on carbon steel. *Materials & Design*. 2012; 41:282-288. <http://dx.doi.org/10.1016/j.matdes.2012.05.008>.
- Narayanan TSNS. Surface pretreatment by phosphate conversion coatings: a review. *Materials Science*. 2005; 9:130.
- Weng D, Jokiel P, Uebles A and Boehni H. Corrosion and protection characteristics of zinc and manganese phosphate coatings. *Surface and Coatings Technology*. 1997; 88(1-3):147-156. [http://dx.doi.org/10.1016/S0257-8972\(96\)02860-5](http://dx.doi.org/10.1016/S0257-8972(96)02860-5).
- Gentil V. *Livros técnicos e científicos*. Rio de Janeiro: Editora S.A.; 1994.
- Li R, Yu Q, Yang C, Chen H, Xie G and Guo J. Innovative cleaner production for steel phosphorization using Zn–Mn phosphating solution. *Journal of Cleaner Production*. 2010; 18(10-11):1040-1044. <http://dx.doi.org/10.1016/j.jclepro.2010.01.019>.
- Lin S-S. Effect of fibered morphology on the properties of Al₂O₃ nanoceramic films. *Ceramics International*. 2013; 39(3):3157-3163. <http://dx.doi.org/10.1016/j.ceramint.2012.09.099>.
- Hafez HS and El-Fadaly E. Synthesis, characterization and color performance of novel Co²⁺-doped alumina/titania nanoceramic pigments. *Spectrochimica Acta. Part A: Molecular Spectroscopy*. 2012; 95:8-14. <http://dx.doi.org/10.1016/j.saa.2012.04.072>.
- Mohammadloo HE, Sarabi AA and Alvani AAS, Sameie H and Salimi R Nano-ceramic hexafluorozirconic acid based conversion thin film: Surface characterization and electrochemical study. *Surface and Coatings Technology*. 2012; 206:4132-4139. <http://dx.doi.org/10.1016/j.surfcoat.2012.04.009>.
- Droniou P, Fristad WE and Liang J-L. Nanoceramic-based conversion coating. *Metal Finishing*. 2005; 103(12):41-43. [http://dx.doi.org/10.1016/S0026-0576\(05\)80849-9](http://dx.doi.org/10.1016/S0026-0576(05)80849-9).
- Chen TT, Ke ST, Liu YM and Hou KH. The study on optimizing the zinc-phosphate conversion coating process and its corrosion resistance. *Journal of Chung Cheng Institute of Technology*. 2006; 34(2):1-11.
- Tamura H. The role of rusts in corrosion and corrosion protection of iron and steel. *Corrosion Science*. 2008; 50(7):1872-1883. <http://dx.doi.org/10.1016/j.corsci.2008.03.008>.
- American Society for Testing and Materials - ASTM. *ASTM D3359-09: standard test methods for measuring adhesion by tape test*. West Conshohocken; 2009.
- American Society for Testing and Materials - ASTM. *ASTM D 2794-99: standard test method for resistance of organic coatings to the effects of rapid deformation (impact)*. West Conshohocken; 2010.
- Associação Brasileira de Normas Técnicas – ABNT. *ABNT NBR 10545-88: tintas: determinação da flexibilidade por mandril cônico: método de ensaio*. Rio de Janeiro; 1988.
- American Society for Testing and Materials - ASTM. *ASTM B 117-07: standard practice for operating salt spray*. West Conshohocken; 2007.
- American Society for Testing and Materials - ASTM. *ASTM D 714-02: standard test method for evaluating degree of blistering of paints*. West Conshohocken; 2009.

18. American Society for Testing and Materials - ASTM. *ASTM D 610-08: standard practice for evaluating degree of rusting on painted steel surfaces*. West Conshohocken; 2012.
19. Moore R and Dunham B. Zirronization™: the future of coating pretreatment processes. *Metal Finishing*. 2008; 106(7-8):46-55. [http://dx.doi.org/10.1016/S0026-0576\(08\)80259-0](http://dx.doi.org/10.1016/S0026-0576(08)80259-0).
20. Banczek EP, Terada M, Rodrigues PRP and Costa I. Study of an alternative phosphate sealer for replacement of hexavalent chromium. *Surface and Coatings Technology*. 2010; 205(7):2503-2510. <http://dx.doi.org/10.1016/j.surfcoat.2010.09.053>.
21. Banczek EP, Rodrigues PP and Costa I. The effects of niobium and nickel on the corrosion resistance of the zinc phosphate layers. *Surface and Coatings Technology*. 2008; 202(10):2008-2014. <http://dx.doi.org/10.1016/j.surfcoat.2007.08.039>.
22. Wang P, Zhang D, Qiu R and Hou B. Super-hydrophobic film prepared on zinc as corrosion barrier. *Corrosion Science*. 2011; 53(6):2080-2086. <http://dx.doi.org/10.1016/j.corsci.2011.02.025>.
23. Feng A, McCoy BJ, Munir ZA and Cagliostro D. Wettability of transition metal oxide surfaces. *Materials Science and Engineering*. 2011; 50:A242.
24. Bombara G and Bernabai U. On surface factors affecting the protectiveness of organic coatings on phosphatized steel. *Surface Technology*. 1980; 11(6):393-401. [http://dx.doi.org/10.1016/0376-4583\(80\)90100-4](http://dx.doi.org/10.1016/0376-4583(80)90100-4).
25. Lampin M, Warocquier-Clérout R, Legris C, Degrange M and Sigot-Luizard MF. Correlation between substratum roughness and wettability, cell adhesion, and cell migration. *Journal of Biomedical Materials Research*. 1997; 36(1):99-108. [http://dx.doi.org/10.1002/\(SICI\)1097-4636\(199707\)36:1<99::AID-JBM12>3.0.CO;2-E](http://dx.doi.org/10.1002/(SICI)1097-4636(199707)36:1<99::AID-JBM12>3.0.CO;2-E). PMID:9212394
26. Li XM, Reinhoudt D and Crego-Calama M. What do we need for a superhydrophobic surface? A review on the recent progress in the preparation of superhydrophobic surfaces. *Chemical Society Reviews*. 2007; 36(8):1350-1368. <http://dx.doi.org/10.1039/b602486f>. PMID:17619692
27. Bajat JB, Popić JP and Mišković-Stanković VB. The influence of aluminium surface pretreatment on the corrosion stability and adhesion of powder polyester coating. *Progress in Organic Coatings*. 2010; 69(4):316-321. <http://dx.doi.org/10.1016/j.porgcoat.2010.07.004>.
28. Adhikari S, Unocic KA, Zhai Y, Frankel GS, Zimmerman J and Fristad W. Hexafluorozirconic acid based surface pretreatments: Characterization and performance assessment. *Electrochimica Acta*. 2011; 56(4):1912-1924. <http://dx.doi.org/10.1016/j.electacta.2010.07.037>.
29. Jegdić BV, Bajat JB, Popić JP and Mišković-Stanković VB. The EIS investigation of powder polyester coatings on phosphated low carbon steel: the effect of NaNO₂ in the phosphating bath. *Corrosion Science*. 2011; 53(9):2872-2880. <http://dx.doi.org/10.1016/j.corsci.2011.05.019>.